ROYAL SOCIETY OF CHEMISTRY

Journal Name

ARTICLE

Reactivity of Parent Amido Complexes of Iridium with Olefins: C−NH₂ Bond Formation *versus* C−H Activation

Inmaculada Mena,[a] Pilar García-Orduña,[a] Víctor Polo,[b] Fernando J. Lahoz,[a] Miguel A. Casado[a],* and Luis A. Oro[a,c]

Herein we report on the different chemical reactivity displayed by two mononuclear terminal amido compounds depending on the nature of the coordinated diene. Hence, treatment of amido-bridged iridium complexes [{Ir(μ-NH₂)(tfbb)}₃] (**1**; tfbb = tetrafluorobenzobarrelene) with dppp (dppp = bis(diphenylphosphane)propane) leads to the rupture of the amido bridges forming in a first stage the mononuclear terminal amido compound [Ir(NH₂)(dppp)(tfbb)] (**3**). On changing the reaction conditions, the formation of a C−NH₂ bond between the amido moiety and the coordinated diene is obtained and a new dinuclear complex [{Ir(1,2-η²-4-κ-C₁₂H₈F₄N)(dppp)}₂(μ-dppp)] (**4**) is isolated. On the contrary, the diiridium amido-bridged complex [{Ir(μ-NH₂)(cod)}₂] (**2**; cod = 1,5-cyclooctadiene) in the presence of dppb (dppb = bis(diphenylphosphane)butane) allows the isolation of a mononuclear complex [{Ir(1,2,3-η³-6-κ-C₈H₁₀)H(dppb)}] (**5**), as a consequence of the extrusion of ammonia. The monitoring of the reaction of **2** with dppb (and dppp) allowed us detecting terminal amido complexes [Ir(NH₂)(P−P)(cod)] (P−P = dppb (**6**), dppp (**7**)) in solution, as confirmed by an X-ray analysis of **7**. Complex **7** was observed to evolve to hydrido species **5** at room temperature. DFT studies showed that the C−H bond activation occurs through the deprotonation of one methylene fragment of the cod ligand by the highly basic terminal amido moiety instead of C−H oxidative addition to the Ir(I) center.

Introduction

N–H activation of ammonia by late metal complexes is an issue of current interest, especially regarding the context of its catalytic functionalization.[1] From an organometallic perspective, interaction of ammonia with well-designed metallic precursors may lead to the formation of amido late metal reactive species. In this way, the utilization of robust pincer-like ligand architectures in combination with iridium allows the homolytic activation of the N–H bond of ammonia, rendering hydrido terminal amido complexes.[2] A parallel approach based on metal-ligand cooperation has enlighten a novel heterolytic mechanism operative in the activation of the N−H bond of NH₃, leading to the formation of terminal amido complexes of ruthenium(II),[3] iridium(I)[4] and nickel(II),[5] where the metals do not change their oxidation states during the activation processes. These

and other[6] approaches have allowed some access to a source of parent-amido complexes of late metals.

The reactivity of terminal late metal parent-amido [M−NH₂] complexes of ruthenium has been studied in some detail and so far it includes the study of proton exchange processes,[7] insertion of carbon monoxide into the N−H bond of the amido fragment[8] and reductive elimination of ammonia,[9] a work that highlights the high basicity at the terminal amido fragment bearing a reactive free electron pair at the nitrogen atom. Also, migratory insertion of olefins into M−N bonds is a common step in amination reactions involving the formation of C−N bonds (see Scheme 1a).[10] The situation changes drastically when the amido moieties act as bridges, where the lone electronic pair is usually tightly bounded in a dative fashion to a second metal.[11] In this line we reported the facile preparation of bridged-amido polynuclear complexes of iridium and rhodium through the heterolytic N−H activation of ammonia induced by methoxo-bridged complexes.[12] These amido complexes have been the body of an intense research directed to understand the chemical reactivity of these rare species.[13] For instance, a significant contribution has been recently reported dealing with the role of [Ir−NH₂−Ir] linkages in catalytic transfer hydrogenation, enlightening a novel binuclear, outer-sphere Noyori-like mechanism, in which the NH₂ groups behave as non-innocent ligands playing a key role in alcohol dehydrogenation and imido formation.[14]

[a.] *Instituto de Síntesis Química y Catálisis Homogénea ISQCH, Universidad de Zaragoza-CSIC, C/Pedro Cerbuna, 12, 50009, Zaragoza, Spain. Fax: 34 976 761 187; Tel: 34 876 553 502. E-mail: mcasado@unizar.es*
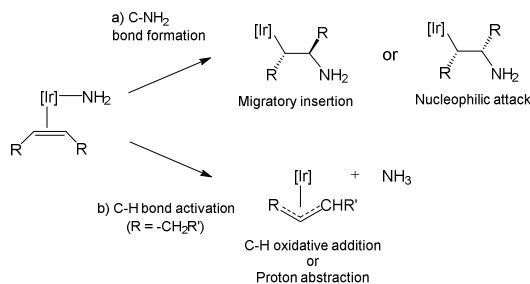
[b.] *Departamento de Química Física e Instituto de Biocomputación y Física de Sistemas Complejos (BIFI), Universidad de Zaragoza, 50009, Zaragoza, Spain*

[c.] *Center for Refining & Petrochemicals King Fahd University of Petroleum & Minerals, Dhahran, 31261, Saudi Arabia*

ARTICLE

Journal Name

Scheme 1 Possible mechanistic pathways for reactions of iridium amido complexes with olefins.

We recently reported the reactivity involved with trinuclear amido-bridged complex [{Ir(μ-NH$_2$)(tfbb)}$_3$] (**1**; tfbb = tetrafluorobenzobarrelene) and simple phosphanes (PEt$_3$, PPhMe$_2$, PPh$_2$Me), which resulted in an original C–NH$_2$ bond formation between the amido fragments and the coordinated diolefin (see Scheme 1a). DFT studies performed on those transformations indicate that the C–N bond formation process is based on a nucleophilic attack of the amido moiety to a diene coordinated to a neighbouring molecule by means of a bimolecular mechanism induced by the high basicity of the amido fragment.[15] In an effort to extend this chemistry, herein we report on the reactivity of several amido-bridged diolefin iridium complexes with bis(phosphanes), which seems to be governed by the nature of the diene attached to the metal. Hence, in addition to C–NH$_2$ bond formation, C–H bond activation processes are found and presented in this work (see Scheme 1b) where the reaction mechanism is rationalized on the basis of DFT calculations.

Results and discussion

C–NH$_2$ bond formation

Addition of bis(diphenylphosphane)propane (dppp) to a C$_6$D$_6$ solution of trinuclear amido complex [{Ir(μ-NH$_2$)(tfbb)}$_3$] (**1**) in a 3:1 molar ratio gave a red suspension, whose ^{31}P{^{1}H} NMR spectrum showed the formation of an iridium complex **3** characterized by a sole resonance at −14.2 ppm. The ^{1}H NMR spectrum of the reaction mixture showed, along with some free tfbb, a simple pattern of resonances in which the tfbb protons were observed at 5.24 pm (CH) and 2.38 ppm (=CH); most interestingly, a broad resonance observed at −0.17 ppm was assigned to an iridium-amido fragment, where the ratio of tfbb:dppp:NH$_2$ observed was 1:1:1 (See Fig. S1). On the contrary, the use of the bis(phosphane) dppb under the same experimental conditions in conjunction with **1** formed highly insoluble solids that were not possible to characterize in solution. In this line, the low solubility of compound [Ir(NH$_2$)(dppp)(tfbb)] (**3**) precluded a deeper characterization in solution, while all the attempts made in order to isolate it failed and only mixtures of P-containing products were obtained, most probably decomposition products, a likely scenario for highly reactive terminal amido complexes of late metals.

In an attempt to increase the solubility of complex **3** we carried out the reaction of **1** with dppp in chloroform; the completion of the process required a slight excess of dppp (NMR evidence) and a white solid **4** was isolated in moderate yields. The spectroscopic characterization of **4** indicated a substantial change in the outcome of the reaction (Scheme 2). Firstly, the ^{31}P{^{1}H} NMR spectrum of **4**

showed three well-separated complex resonances, which in principle indicated the presence of three chemically non-equivalent phosphorus nuclei in the molecule (Fig. S4); additionally the pattern of the ^{1}H NMR spectrum of **4** showed that the original tfbb molecule changed throughout the transformation. However, the low solubility of complex **4** precluded a deeper characterization in solution. We managed to grow a single crystal of complex **4** which was subsequently studied by X-ray crystallographic methods. The molecular structure of compound [{Ir(1,2-η^2-4-κ-C$_{12}$H$_8$F$_4$N)(dppp)}$_2$(μ-dppp)] (**4**) is depicted in Fig. 1 together with the most significant bond distances and angles.
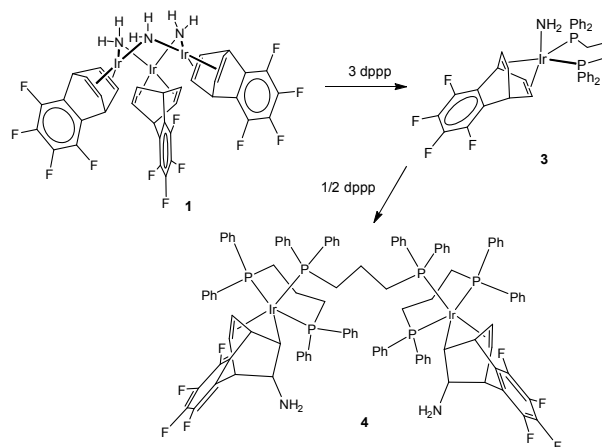
Scheme 2 Synthesis of complexes **3** and **4**.

The solid state structure reveals that compound **4** is a dinuclear complex, formed by two [Ir(dppp)(1,2-η^2-4-κ-tfbb derivative)] organometallic fragments linked together through a dppp ligand. Metal environment, bond distances and angles around both metal atoms are analogous, and a non-crystallographic C_2 symmetry (with the 2-fold axis parallel to y axis and passing through C53 carbon atom) is observed between both mononuclear subunits. The coordination of metal atoms involves three phosphorus atoms (two of a chelate dppp molecule and other from the bridging dppp ligand) and a tfbb-derivative fragment occupying the remaining two coordination sites with a 1,2-η-4-κ coordination mode. Each pentacoordinated iridium atom exhibits a distorted trigonal bipyramidal geometry. The equatorial plane is formed by two P atoms from different dppp moieties (P1 and P3; P4 and P6 for Ir1 and Ir2, respectively), and the olefinic bond of the carbocyclic ligand (C1=C2, C55=C56). Apical positions are fulfilled by a phosphorous atom (P2 and P5) and the κ-C5 (κ-C59) metallated carbon of the carbocycle, with P-Ir-C angles of 163.6(3) and 163.2(3)°.

Journal Name

ARTICLE
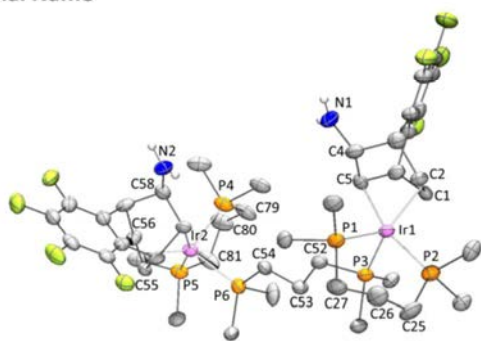
Fig. 1 Molecular structure of complex **4**. For clarity, only the *ipso* carbon atoms of the phenyl groups have been depicted and hydrogen atoms (except those of NH₂) have been omitted. Selected bond distances (Å) and angles (°) for **4**: Ir1–P1 2.314(2), Ir1–P2 2.318(3), Ir1–P3 2.350(3), Ir2–P4 2.322(2), Ir2–P5 2.331(2), Ir2–P6 2.331(3), Ir1–C5 2.163(9), Ir2–C59 2.155(9), Ir1–Ct1[a] 1.991(8), Ir2–Ct2[a] 2.017(8), P1-Ir1-P2 94.10(9), P1-Ir1-P3 97.67(9), P4-Ir2-P5 92.66(9), P4-Ir2-P6 96.55(10), P1-Ir1-C5 95.7(2), P4-Ir2-C59 95.0(2), P1-Ir1-Ct1 128.7(2), P4-Ir2-Ct2 132.8(2), P2-Ir1-P3 95.85(8), P5-Ir2-P6 100.58(9), P2-Ir1-C5 163.6(3), P5-Ir2-C59 163.2(3), P2-Ir1-Ct1 97.8(2), P5-Ir2-Ct2 97.8(3), P3-Ir1-C5 95.9(3), P6-Ir2-C59 93.4(3), P3-Ir1-Ct1 130.1(3), P6-Ir2-Ct2 126.0(2). [a] Ct1 and Ct2 are the centroids of C1=C2 and C55=C56 olefinic bonds, respectively.

The P3-C52-C53-C54-P6 backbone of the bridging dppp ligand is planar and nearly coplanar to Ir atoms, leading to a large intermetallic separation (9.1561(8) Å) which precludes any Ir···Ir interaction. This disposition differs with previously reported examples of dppp molecules bridging two iridium atoms[16] where the metal is also linked through additional ligands, giving rise to cyclic situations and shortest Ir···Ir distances (2.77 Å[16b,c] or 5.620(1)[16a] Å).

The most striking feature of the molecule is the presence of a newly formed carbocycle, 1,2-η-4-κ-coordinated to iridium and further functionalized with an –NH₂ amino fragment at the C4 sp³-carbon at the *exo* site. In this line, we have already reported the coupling of the –NH₂ fragment to the apical olefin in [Ir(1,2-η²-4-κ-C₁₂H₈F₄N)(PMePh₂)₃]. The bond lengths characterizing this coordination (2.011(4) and 2.157(4) Å)[15] nicely agree with those found in complex **4** (Ir–Ct: 1.991(8) and 2.017(8) Å and Ir–C: 2.163(9) and 2.155(9) Å).

Once the molecular structure of **4** has been enlighten, the inspection of the multinuclear NMR spectra revealed that its structure was maintained in solution; the patterns of resonances observed in both the ¹H NMR and ³¹P{¹H} NMR spectra were comparable to those shown by the mononuclear version [Ir(1,2-η²-4-κ-C₁₂H₈F₄N)(PR₃)₃] (PR₃ = PEt₃, PMePh₂, PMe₂Ph).[15] More specifically, the ¹H NMR spectrum of **4** showed the tfbb derivative as six well-separated resonances, while the –NH₂ fragment was observed at 0.03 ppm (See Fig. S3 and the Experimental Section). The low solubility of **4** in most organic solvents precluded the acquisition of a ¹³C{¹H}-APT NMR spectrum; however, the mass spectrum of **4** gave an intense peak at *m/z*: 2016.149, which corresponded to the molecular ion minus a proton, and microanalytical data agreed with the composition of the compound.

The *exo* stereochemistry of the –NH₂ fragment in complex **4** clearly signals for a nucleophilic attack of the amido fragment rather than migratory insertion. For a related complex, a DFT study showing the feasibility of a bimolecular nucleophilic attack of a metal amido to the coordinated olefin was published previously by Mena *et al.*[15]

C–H bond activation

Next we shifted to the known dinuclear amido-bridged complex [{Ir(μ-NH₂)(cod)}₂] (**2**; cod = 1,5-cyclooctadiene)[12a] and studied its interaction with selected bis(phosphanes). Treatment of **2** with dppp in toluene at room temperature gave an intractable mixture of P-containing iridium complexes; however, reaction of **2** with dppb under the same experimental conditions afforded a light yellow solid further characterized as the mononuclear hydrido complex [{Ir(1,2,3-η³-6-κ-C₈H₁₀)H(dppb)] (**5**; Scheme 3). The ¹H NMR spectrum of **5** in C₆D₆ showed the hydrido ligand as a triplet at high field, with a coupling constant ($^2J_{H–P}$ = 18.7 Hz) that located it *cis* to the phosphorus atoms from dppb. Additionally, five well-separated complex resonances were observed at low field; the ones located at lower field indicated the presence of a non-coordinated olefin. The remaining three signals corresponded to an allyllic fragment η³-coordinated to iridium. Through a combination of NMR techniques, including ¹H-¹H COSY, ¹H-¹³C HSQC and ¹H-¹H NOESY bidimensional experiments (See the Supporting Information), we were able to figure out the composition and connectivity of the new carbocycle in complex **5**, which is shown in Scheme 3. The analysis of the NMR data of **5** in solution clearly indicated that the initial η⁴-coordinated cod ligand in **2** has undergone a drastic transformation becoming a 1,2,3-η³-6-κ-C₈H₁₀ carbocycle fragment coordinated to iridium in **5**, a proposal further confirmed by X-ray methods.
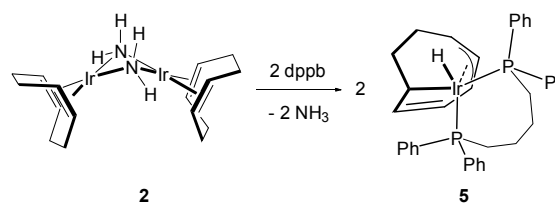

Scheme 3 Synthesis of hydrido complex **5**.

We managed to grow pale yellow single crystals of complex [{Ir(1,2,3-η³-6-κ-C₈H₁₀)H(dppb)] (**5**) that were subjected to an X-ray diffraction analysis. Molecular structure of compound **5** is depicted in Fig. 2, together with the most relevant bond distances and angles. The iridium(III) metallic center shows a severely distorted octahedral geometry where the carbocyclic molecule occupies three coordination sites, the bis(phosphane) is coordinated through both phosphorus atoms and a hydrido ligand completes the coordination sphere. The equatorial plane is defined by the phosphorous atoms of the dppb ligand, one terminal allyl carbon atom (C1), and the Ir–C carbon atom (C6), while the apical positions are occupied by the other terminal allyl carbon atom (C3) and the hydrido ligand. The Ir–P1 bond distance is 0.0365(14) Å longer than that of Ir–P2 bond as a consequence of the higher *trans* effect exerted by the C6 metallated carbon atom. Focusing on the η³ coordination mode of the carbocyclic ligand, the Ir–C2 bond length is the shortest Ir–C(allyl) bond distances, reflecting the typical metal π-allyl coordination in which the central carbon atom is closer to the metal.[17] The Ir–C6 bond separation (2.154(4) Å) is slightly longer

ARTICLE **Journal Name**

than those found in other metallated complexes such as [Ir(PNP)(κ^1-η^2-C_8H_{13})(H)] (2.109(5) Å; PNP = $^nPrN(CH_2CH_2PPh_2)_2$)[18] and [{Ir(κ^1-η^3-C_8H_{12})H(dppm)}] (2.115(6) Å).[17a] It should be remarked that the C4−C5 bond distance (1.309(6) Å) corresponds to that of a double C=C bond. It is important to stress that the carbocyclic fragment in **5** is formed as a consequence of a double C−H bond activation of the cod ligand, a transformation never reported before.
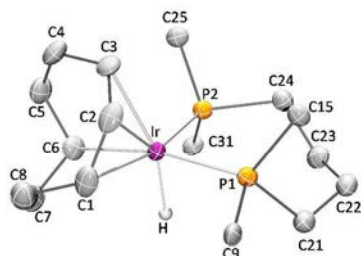

Fig. 2 Molecular structure of complex **5**. For clarity, only the *ipso* carbon atoms of the phenyl groups have been depicted and hydrogen atoms (except hydride ligand) have been omitted. Selected bond distances (Å) and angles (°) for **5**: Ir−P1 2.3071(10), Ir−P2 2.2706(10), Ir−C1 2.211(4), Ir−C2 2.185(4), Ir−C3 2.297(4), Ir−C6 2.154(4), Ir−H 1.53(4), C1−C2 1.460(6), C2−C3 1.417(6), C3−C4 1.486(6), C4−C5 1.309(6), C5−C6 1.497(6), C6−C7 1.514(6), C7−C8 1.532(7), C8−C1 1.529(6), P1-Ir-P2 96.26(4), P2-Ir-H 90.5(16), P1-Ir-C1 96.78(12), C1-Ir-C2 38.80(17), P1-Ir-C2 89.77(12), C1-Ir-C3 68.87(17), P1-Ir-C3 109.40(12), C1-Ir-C6 78.50(17), P1-Ir-C6 168.26(12), C1-Ir-H 96.0(16), P1-Ir-H 83.0(16), C2-Ir-C3 36.75(16), P2-Ir-C1 166.05(13), C2-Ir-C6 93.00(17), P2-Ir-C2 136.47(12), C2-Ir-H 133.0(16), P2-Ir-C3 102.01(12), C3-Ir-C6 79.14(17), P2-Ir-C6 89.58(12), C3-Ir-H 161.0(16).

Therefore complex **5** can be described as the product resulting from net loss of ammonia in the system composed by complex **2** and dppb. In order to get a deeper insight into the mechanism operative in the aforementioned transformation we monitored the reaction of amido-bridged complex **2** with dppb in a Young NMR pressure tube by NMR techniques at variable temperature. The multinuclear NMR spectra of the reaction mixture at −50 °C showed complete conversion within a minute to new species further characterized as the mononuclear amido complex [Ir(NH$_2$)(cod)(dppb)] (**6**). In this way, the ^1H NMR spectrum of **6** in CD$_2$Cl$_2$ at −50 °C showed a significant triplet at δ −3.3 ppm with a small coupling constant that signalled the presence of a terminal amido moiety (Ir−NH$_2$) located *cis* to the phosphorus atoms of dppb; the ^1H-^{15}N HMQC spectrum of **6** located the amido nitrogen atom at −63.6 ppm, a negative value comparable to those found in other terminal parent amido complexes of rhodium.[12a] The olefinic protons of the cod ligand were observed as a broad resonance (δ(^1H) 2.86 ppm) characteristic of a natural η^4-*C=C* coordination to the metal, while the corresponding olefinic carbon atoms gave a broad resonance at 66.8 ppm in the $^{13}C\{^1H\}$-APT NMR spectra of **6** at −50 °C. The $^{31}P\{^1H\}$ NMR spectra of **6** showed the presence of symmetrical species characterized by the presence of a sole singlet throughout all ranges of temperature (0 °C → −90 °C).

The spectroscopic information gathered in solution at low temperatures is coherent with the formation of a mononuclear complex, most probably with a trigonal bipyramidal geometry at all ranges of temperature, in which the apical site should be occupied by the terminal amido fragment and the dppb ligand coordinated at the equatorial plane, while the cod ligand is η^4-*C=C* coordinated at apical and equatorial sites. However this structural situation would render the =CH cod fragments chemically non-equivalent both in the ^1H and the $^{13}C\{^1H\}$ NMR spectra of **6**, a situation that indicates that the complex undergoes a fluxional process in solution that could not be frozen even at −90 °C in CD$_2$Cl$_2$, behaviour often found for stereochemical non-rigid pentacoordinated transition metal complexes.[19] When reaching room temperature, however, transient species **6** has a short existence and it gradually evolved to the clean formation of hydrido complex **5** and free ammonia, as confirmed by NMR methods (Scheme 4). It was not possible to observe any other intermediate species in the transformation **6** → **5**.
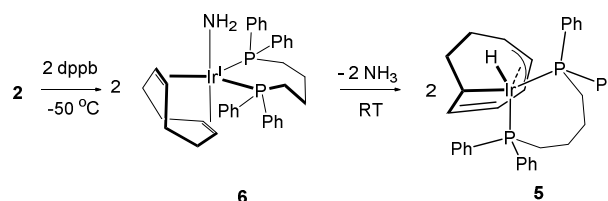
Scheme 4 Formation of hydrido complex **5** *via* terminal amido species **6**.

Unfortunately all the attempts carried out intended to grow single crystals of amido complex **6** were unsuccessful. However the use of the bis(phosphane) dppp in combination with amido complex **2** allowed us to prepare, at low temperatures, the analogous terminal amido complex [Ir(NH$_2$)(cod)(dppp)] (**7**), which turned to be more insoluble than complex **6**. This circumstance helped us on growing a single crystal of intermediate species **7** at low temperature, which was subjected to an X-ray analysis by diffraction methods. The molecular structure of complex **7**, isolated as the ammonia adduct [Ir(NH$_2$)(cod)(dppp)]·NH$_3$ (**7·NH$_3$**) is shown in Fig. 3.
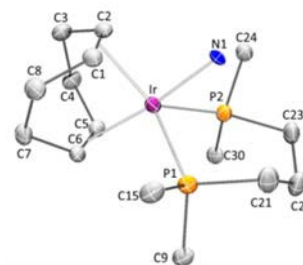
Fig. 3 Molecular structure of complex **7**. Only the *ipso* carbon atoms of the phenyl groups have been depicted and hydrogen atoms have been omitted, for clarity. Selected bond distances (Å) and angles (°) for **7**: Ir−P1 2.3286(6), Ir−P2 2.3769(6), Ir−N1 2.0790(18), Ir−Ct1ᵃ 1.989(3), Ir−Ct2ᵃ 2.043(2), P1-Ir-P2 91.28(2), P1-Ir-N1 85.23(6), P1-Ir-Ct1 129.47(8), P1-Ir-Ct2 99.59(7), P2-Ir-N1 79.87(6), P2-Ir-Ct1 136.17(8), P2-Ir-Ct2 104.68(7), N1-Ir-Ct1 87.40(10), N1-Ir-Ct2 173.20(9), Ct1-Ir-Ct2 85.83(11).

Adduct **7·NH$_3$** is a mononuclear complex whose iridium(I) centre exhibits a slightly distorted trigonal-bipyramidal geometry. The overall geometry of the metal coordination sphere is similar to that found in [Ir(CH$_3$)(cod)(dppp)].[20] The equatorial sites are occupied by

Journal Name

ARTICLE

the phosphorous atoms of the dppp ligand and an olefinic bond of the cod fragment, while the axial positions are filled with the other olefinic bond of the cod ligand and a terminal amido moiety. The geometrical arrangement of the ligands seems to affect the coordination of the cod fragment. Although the chelating diolefin shows its usual η^4-$C=C$ coordination mode, a comparison of the solid-state structures of complexes **7·NH₃** and **2** evidences dissimilarities between Ir–Ct bond lengths in the former while they are statistically equal in the later**,** together with slightly smaller bite angle (**7·NH₃**: 85.83(11)°, mean value in **2**: 88.2(1)°).[13a]

Iridium-phosphorous bond lengths are not equivalent. A longer value is found involving the phosphorous atom which is more nearly *trans* to the olefinic bond situated at the equatorial plane (P2-Ir-Ct1: 136.17(8)°, P1-Ir-Ct1: 129.47(8)°), with similar bond angles to those observed in [Ir(CH₃)(cod)(dppp)] (135.4(5) and 128.7(5)°).[20] The Ir–N1 bond distance (2.0790(18) Å) deserves further remarks. Although so far the characterized molecular structures featuring a terminal parent amido moiety [Ir–NH₂] are quite scarce, they span different ligands and metal coordination geometries. Ir–N bond length in compound **7·NH₃** is found to be longer than those of those of trigonal bipyramidal [(D^{t}BPP)IrH(NH₂)][2a] (1.999(4) Å) and square planar complexes with PNP[6b] and NNN[21] pincer ligands (1.954(4)-1.900(2) Å), shorter than that found in octahedral complex [(η³-C₆H₃-2,6-(CH₂P^{t}Bu₂)₂Ir(^{t}BuNC)H(NH₂)][9] (2.193(4) Å) and similar to that of octahedral [Cp*Ir(PMe₃)(Ph)(NH₂)][22] complex (2.105(8) Å) where an absence of π-bonding interaction has been reported.

Hydrogen atoms bonded to amido nitrogen were observed in Fourier difference maps, but their refinement did not properly converge. Therefore, they have not been included in the model and the X-ray diffraction data of compound **7·NH₃** does not allow a precise characterization of the hydrogen bond interaction. However, the short 2.662(9) Å separation between both amido and ammine nitrogen atoms suggests the existence of this bonding interaction.

The spectroscopic data obtained in the multinuclear NMR spectra of adduct **7·NH₃** is readily comparable to those observed for the analogue dppb derivative **6**. However, an additional resonance was observed at −1.53 ppm in the ^{1}H NMR spectrum of **7·NH₃**, which correlated with a signal at −33.6 ppm in the ^{1}H-^{15}N HMBC NMR spectrum, tentatively assigned to the ammonia molecule interacting with the Ir−NH₂ moiety, which showed crossed peaks with free ammonia in the ^{1}H-^{1}H NOESY NMR spectrum (See Fig. S16).

DFT studies

In order to gain more insight on the transformation of the terminal parent-amido [M−NH₂] complex **6** into hydrido compound **5** and ammonia a detailed mechanistic study using DFT methodology at the B3LYP-D3(PCM)/def2-TZVP//B3LYP-D3/def2-SVP level has been carried out. The calculated Gibbs energetic profile is shown in Fig. 4. Starting at **6** (labelled **A**), two possible mechanistic pathways can be envisioned for the hydrogen abstraction from the cod and release of an ammonia molecule. The first entails the oxidative addition of one C−H bond of the cod ligand to the metal, leading to an hydrido intermediate **B** (Fig. 4, red path) while the second consists of the direct deprotonation of the cod by the amido group without participation of the metal (Fig. 4, blue path). The former proposal is characterized by the **TSAB** transition state which presents an energetic barrier of 33.4 kcal mol^{-1}, being unaffordable for the current experimental conditions. The proposed Ir(III) hydrido intermediate (**B**) is relatively stable (18.5 kcal mol^{-1}). However, reductive elimination of ammonia from **B** presents also a very high energetic barrier (37.7 kcal mol^{-1}). The alternative pathway requires the initial decoordination of one of cod double bonds from the metal, a process that leads to square-planar intermediate **A'** which is 18.2 kcal mol^{-1} less stable than the trigonal bipyramidal complex **A**. Then, proton transfer from a methylene group adjacent to the coordinated olefin to the lone electron pair of the amido group requires an affordable energetic barrier of 22.2 kcal mol^{-1} (**TSA'C**), much lower than the previous alternative pathway. Both routes converge to intermediate **C** which features an ammonia ligand and is 16.2 kcal mol^{-1} less stable than **A** and the deprotonated cod shows a η^1 coordination to the metal. Ammonia can be released at this stage and the metal coordinates in η^3 fashion to the deprotonated carbocycle, forming intermediate **D** which is slightly exergonic (−4.9 kcal mol^{-1}). Finally, the Ir(III) hydrido species **E** (corresponding to complex **5**) may be obtained upon oxidative addition of a cod C−H bond by the metal through **TSDE** transition state which presents an energetic barrier of 21.7 kcal mol^{-1} forming the exergonic product **E**, −10.3 kcal/mol.

ARTICLE

Journal Name
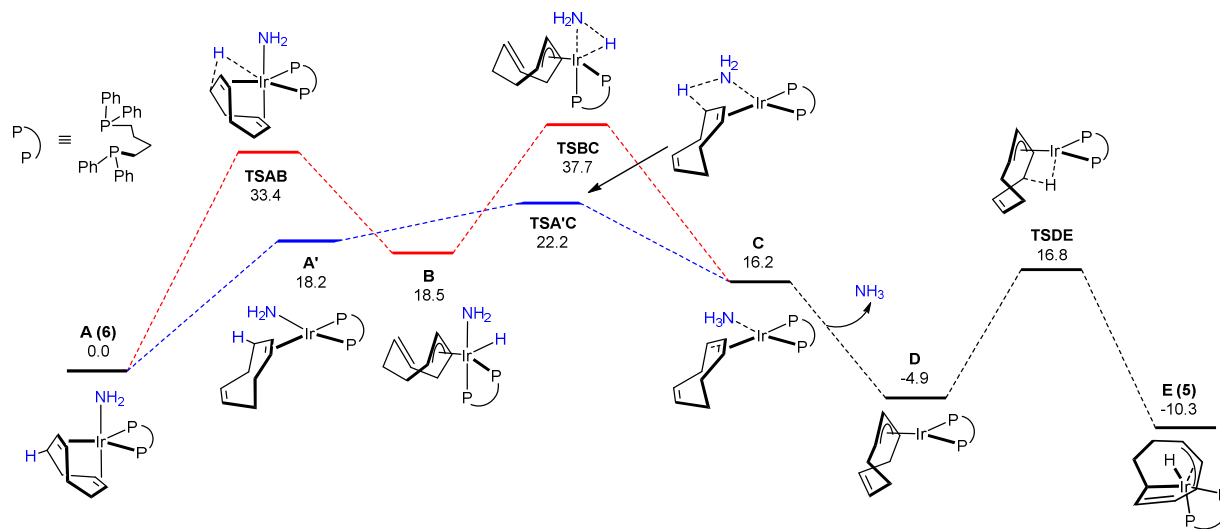
Fig. 4 DFT calculated Gibbs energy reaction profile (in Kcal/mol, relative to **A**) for the conversion of metal amido complex **6** into **5** and ammonia.

Conclusions

In this contribution we have shown different reactivity patterns of polynuclear amido-bridged iridium(I) complexes when interacting with bis(phosphanes), which strongly depend on the nature of the diolefinic ancillary ligands (tfbb vs. cod). Both trinuclear and dinuclear amido-bridged complexes bearing the diolefins tfbb and cod, respectively, react in a first stage with a given bis(phosphane) affording rare, terminal parent amido mononuclear species that arise as a consequence of bridge splitting. From here, mainly electronic issues concerning the coordinated diene molecules seem to govern the reactivity of the terminal $-NH_2$ moieties. The tfbb-containing iridium complex undergoes an intermolecular $C-NH_2$ coupling induced by the electronic nature of the diene, leading to an amino-functionalized tfbb derivative which becomes metallated to iridium. On the contrary, the flexible backbone of the cod ligand allows the deprotonation of one of the methylene fragments by the amido group, releasing ammonia and forming an Ir(III) hydrido derivative.

Experimental

General methods: All manipulations were performed under a dry argon atmosphere using Schlenk-tube techniques. Solvents were obtained from a Solvent Purification System (Innovative Technologies) or were dried by standard procedures and distilled under argon prior to use. Complexes **1** and **2** were prepared by following published synthetic procedures.[12a] Gaseous ammonia was purchased from Air Liquide LTD. All the other chemicals used in this work (dppp, dppb) have been purchased from Aldrich Chemicals and used as received. Carbon, hydrogen and nitrogen analyses were performed with a Perkin-Elmer 2400 CHNS/O microanalyzer. Mass spectra were recorded on a VG Autospec double-focusing mass spectrometer operating in the FAB$^+$ mode. Ions were produced with the standard Cs$^+$ gun at ca. 30 kV; 3-nitrobenzyl alcohol (NBA) was used as matrix. ESI-MS were recorded on a Bruker Micro-Tof-Q by using sodium formiate as reference. ^{1}H, ^{31}P$\{^1$H$\}$ and ^{13}C$\{^1$H$\}$ NMR spectra were recorded on a Varian UNITY, Bruker ARX 300, and Bruker Avance 400 spectrometers operating at 299.95, 121.42 and 75.47 MHz, 300.13, 121.49 and 75.47 MHz, and 400.13, 161.99 and 100.00 MHz, respectively. ^{1}H, ^{31}P$\{^1$H$\}$ and ^{13}C$\{^1$H$\}$ spectra were recorded on a Chemical shifts are reported in ppm and referenced to Me$_4$Si using the residual signal of the deuterated solvent (^{1}H and ^{13}C), H$_3$PO$_4$ as external reference (^{31}P) and liquid NH$_3$ (^{1}H-^{15}N HMQC).

***In situ*** characterization of [{Ir(NH$_2$)(dppp)(tfbb)] (3).**
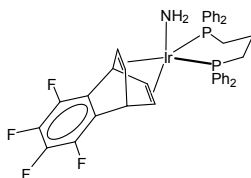
To a solution of **1** (11 mg, 0.08 mmol) in C$_6$D$_6$ (0.5 mL), solid bis(diphenylphosphane)propane (10 mg, 0.024 mmol) was added and the resulting reddish mixture was stirred for 10 min and then it was analysed by NMR techniques. ^{1}H NMR (300 MHz, C$_6$D$_6$): δ = 6.91-7.76 (set of m, 20H, Ph), 5.24 (m, 2H, CH tfbb), 3.50 (m, 2H, CH$_2$ dppp), 2.38 (m, 4H, =CH tfbb), 2.22 (m, 4H, CH$_2$ dppp), −0.17 (m, 2H, NH$_2$); ^{31}P$\{^1$H$\}$ NMR (121 MHz, C$_6$D$_6$): δ = −14.2 (s).

Synthesis of [{Ir(1,2-η^2-4-κ-C$_{12}$H$_8$F$_4$N)(dppp)}$_2$(μ-dppp)] (4).
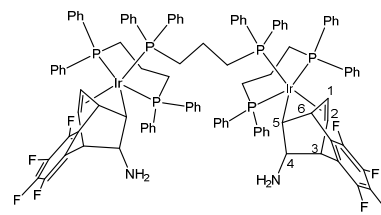
To a solution of **1** (0.08 g, 0.06 mmol) in toluene (8 mL), solid bis(diphenylphosphane)propane (0.11 g, 0.27 mmol) was added and the resulting light orange solution was stirred for 1h at room temperature, where a whitish solid began to crystallize out the solution. The solvent was then removed by vacuum until ca. 1 mL, and further addition of hexanes separated a white solid that was filtered through a cannula, washed with hexanes and then dried under vacuum (0.07 g, 48%). ^{1}H NMR (300 MHz, CDCl$_3$): δ = 7.72 (m, 4H), 6.97-7.45 (set of m, 48H), 6.80 (m, 4H), 6.18 (m, 4H) (PPh$_2$), 4.50 (m, 2H, H^6), 3.76 (m, 2H, H^3), 3.50 (m, 2H, H^4), 2.36 (m, 2H, CH$_2$ dppp), 2.27 (m, 2H, H^5), 2.36 (m, 4H, CH$_2$ dppp), 2.05 (m, 2H, H^2), 1.26 (m, 4H, CH$_2$ dppp), 1.12 (m, 2H, H^1), 0.87 (m, 4H, CH$_2$ dppp), 0.70 (m, 4H, CH$_2$ dppp), 0.03 (m, 4H, NH$_2$); ^{31}P$\{^1$H$\}$ NMR (121 MHz, CDCl$_3$): δ = −20.3 (dd, $^2J_{P-P}$ = 59.1 Hz, $^2J_{P-P}$ = 11.6 Hz), −25.2 (dd, $^2J_{P-P}$ = 59.1 Hz, $^2J_{P-P}$ = 11.6 Hz), −37.9 (t, $^2J_{P-P}$ = 11.6 Hz); MS: μ-TOF$^+$ (Tol/CH$_3$CN): *m/z* 2106.149 [M$^+$ − 1H]; elemental analysis calcd (%) for C$_{105}$H$_{94}$F$_8$N$_2$Ir$_2$P$_6$: C 59.88, H 4.50, N 1.33; found: C 59.64, H 4.31, N 1.28.

Synthesis of [{Ir(1,2,3-η^3-6-κ-C$_8$H$_{10}$)H(dppb)] (5).
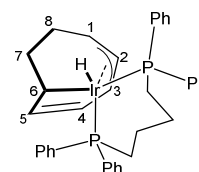
To a solution of **2** (0.08 g, 0.13 mmol) in toluene (8 mL), solid bis(diphenylphosphane)butane (0.11 g, 0.26 mmol) was added and the resulting solution was stirred for 1h at room temperature. The solvent was then removed by vacuum, and further addition of hexanes separated a white solid that was filtered through a cannula, washed with hexanes and then dried under vacuum (0.15 g, 82%). ^{1}H NMR (300 MHz, C$_6$D$_6$): δ = 8.24 (m, 2H, H^o PPh$_2$), 7.53 (m, 2H, H^o PPh$_2$), 6.97-7.42 (set of m, 16H, PPh$_2$), 5.27 (m, 1H, =CH^5), 4.99 (m, 1H, =CH^4), 4.54 (m, 1H, CH^3), 4.14 (m, 1H, CH^2), 3.20 (m, 1H, CH^1), 2.91 (m, 2H, CH$_2$^{7} + CH$_2$), 2.66 (m, 1H, CH^6), 2.51 (m, 1H),

Journal Name

ARTICLE

2.36 (m, 1H) (CH$_2$ dppb), 2.20 (m, 2H, CH$_2^8$ + CH$_2$ dppb), 2.10 (m, 1H, CH$_2^7$), 1.94 (m, 1H, CH$_2$ dppb), 1.77 (m, 2H, CH$_2^8$ + CH$_2$ dppb), 1.13 (m, 2H, CH$_2$ dppb), −11.64 (t, $^2J_{H-P}$ = 18.7 Hz, 1H, Ir−H); ^{31}P{^{1}H} NMR (121 MHz, C$_6$D$_6$): δ = 4.0 (m), −1.2 (m); ^{13}C{^{1}H}-APT NMR (75 MHz, C$_6$D$_6$): δ = 146.1 (=C^{5}H cod), 140.6 (d, $^1J_{C-P}$ = 47 Hz, C^{ipso}), 139.3 (d, $^1J_{C-P}$ = 39 Hz, C^{ipso}), 135.3 (d, $^2J_{C-P}$ = 9 Hz, C^o), 135.1 (d, $^2J_{C-P}$ = 11 Hz, C^o), 134.6 (d, $^1J_{C-P}$ = 29 Hz, C^{ipso}), 133.3 (d, $^1J_{C-P}$ = 47 Hz, C^{ipso}), 131.6 (d, $^2J_{C-P}$ = 8 Hz, C^o), 131.4 (d, $^2J_{C-P}$ = 8 Hz, C^o), 130.1, 129.7, 128.3, 128.0 (all s, C^p), 127.2, 127.1, 127.0, 126.9 (all s, C^m) (PPh$_2$), 126.5 (d, $^3J_{C-P}$ = 5 Hz, =C^{4}H), 89.2 (C^{2}H), 78.8 (=C^{3}H), 65.5 (d, $^2J_{C-P}$ = 34 Hz, C^{1}H), 52.4 (d, $^1J_{C-P}$ = 11 Hz, PCH$_2$), 38.1 (d, $^1J_{C-P}$ = 26 Hz, PCH$_2$), 34.9 (dd, $^3J_{C-P}$ = 30 Hz, $^3J_{C-P}$ = 8 Hz, C^{7}H$_2$), 34.8 (dd, $^2J_{C-P}$ = 74 Hz, $^2J_{C-P}$ = 7 Hz, C^{6}H), 25.3 (CH$_2$), 24.4 (C^{8}H$_2$), 23.0 (CH$_2$); MS: μ-TOF$^+$ (Tol/CH$_3$CN): *m/z* 725.228 [M$^+$ − 1H]; elemental analysis calcd (%) for C$_{36}$H$_{39}$IrP$_2$: C 59.57, H 5.42; found: C 59.32, H 5.37.

***In situ* characterization of [Ir(NH$_2$)(cod)(dppb)] (6).**
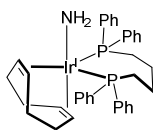
A pressure Young NMR tube was charged with **2** (70 mg, 0.11 mmol), dppb (97 mg, 0.22 mmol) and then it was cooled down to −50 ^{o}C. At this point CD$_2$Cl$_2$ (0.4 mL) was added to form a red solution, and then the reaction tube was sealed and monitored by NMR spectroscopy at low temperatures, which confirmed the total conversion to amido complex **6** within a minute. ^{1}H NMR (300 MHz, CD$_2$Cl$_2$, −50 ^{o}C): δ = 7.23-7.73 (set of m, 20H, PPh$_2$), 3.66 (m, 2H, CH$_2$ dppb), 3.48 (m, 2H, CH$_2$P dppb), 2.86 (m, 4H, =CH cod), 2.34 (m, 2H, CH$_2$ dppb), 1.77-1.90 (set of m, 10H, CH$_2$ cod + CH$_2$ dppb), −3.30 (t, $^3J_{H-P}$ = 4.2 Hz, 2H, Ir−NH$_2$); ^{31}P{^{1}H} NMR (121 MHz, CD$_2$Cl$_2$, −50 ^{o}C): δ = −0.7 (s); ^{13}C{^{1}H}-APT NMR (75 MHz, CD$_2$Cl$_2$, −50 ^{o}C): δ = 139.7 (m, C^{ipso}), 135.4 (m, C^{ipso}), 127.6-133.0 (set of m, C^o + C^m + C^p) (PPh$_2$), 66.8 (br, =CH cod), 27.2 (br, CH$_2$ dppb), 23.2, 21.3 (CH$_2$ cod); ^{15}N−^{1}H HMQC (40 MHz, CD$_2$Cl$_2$, −50 ^{o}C): δ = −63.6 (Ir−NH$_2$).

***In situ* characterization of [Ir(NH$_2$)(cod)(dppp)]·NH$_3$ (7·NH$_3$).**
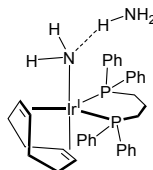
A pressure Young NMR tube was charged with **1** (70 mg, 0.11 mmol) and dppp (91 mg, 0.22 mmol) and then C$_6$D$_6$ (0.4 mL) was added, forming a deep red solution along with the precipitation of a light brown solid that was centrifuged out the solution. This was monitored by NMR spectroscopy at room temperature, where within 2 minutes complex **7·NH$_3$** was formed.^{1}H NMR (300 MHz, C$_6$D$_6$, 0 ^{o}C): δ = 6.72-7.87 (set of m, 20H, PPh$_2$), 3.24 (m, 2H, CH$_2$ dppp), 3.02 (m, 4H, =CH cod), 1.62-2.13 (set of m, 12H, CH$_2$ cod + CH$_2$ dppp), −1.53 (br, 3H, *H$_3$*N···H$_2$N−Ir), −2.70 (t, $^3J_{H-P}$ = 3.6 Hz, 2H, NH$_2$); ^{31}P{^{1}H} NMR (121 MHz, C$_6$D$_6$, 0 ^{o}C): δ = −18.0 (s); ^{13}C{^{1}H}-APT NMR (75 MHz, C$_6$D$_6$, 0 ^{o}C): δ = 135.4-126.8 (set of m, PPh$_2$), 60.0 (t, $^2J_{C-P}$ = 7 Hz, =CH cod), 52.4 (m, CH$_2$P dppp), 33.8, 33.2 (CH$_2$ cod),

28.1 (CH$_2$ dppp); ^{15}N−^{1}H HMQC (40 MHz, toluene-d^8, 0 ^{o}C): δ = −69.7 (Ir−*N*H$_2$), −33.6 (Ir−NH$_2$···−*N*H$_3$).

Crystal Structure Determination of Complexes 4, 5 and 7·NH$_3$. Single crystal X-ray diffraction data were collected at 100(2) K with graphite-monochromated MoKα radiation (λ = 0.71073 Å) using narrow ω rotations (0.3°) on a Bruker SMART APEX (compound **4**) or a Bruker APEX DUO diffractometer (compound **5** and **7·NH$_3$**). SAINT+^{23} and SADABS^{24} programs, integrated in APEX2 package, were used to integrate and correct the absorption effect of the intensities. The structures were solved by direct methods with SHELXS-2013^{25} and refined by full-matrix least-squares refinement in F^2 with SHELXL-2014.^{26}

Crystal data for **4**. C$_{105}$H$_{94}$F$_8$Ir$_2$N$_2$P$_6$·5(C$_7$H$_8$) *M* = 2566.7; colorless prism, 0.118 x 0.146 x 0.148 mm^3; orthorhombic *Fdd2*; *a* = 44.924(2), *b* = 47.578(2), *c* = 21.0515(11) Å; *V* = 44996(4) Å^3; *Z* = 16; ρ_{calc} = 1.516 g cm^{-3}; μ = 2.518 cm^{-1}; min. and max. transmission factors 0.661 and 0.777; 2θ$_{max}$ = 57.566°; 129633 reflections collected; 26983 unique reflections [R_{int} = 0.0648]; number of data/restraints/parameters: 26983/3/1136; final *GOF* 1.080; R_1 = 0.0486 [22357 reflections, *I* > 2σ(*I*)], wR_2 = 0.1084 for all data; largest difference peak: 1.394 e Å^{-3}; Flack parameter **−**0.009(2). Once the model included a dinuclear iridium complex and three toluene molecules, clear evidence of the presence of additional solvent was obtained. An analysis of the solvent region has been performed using SQUEEZE program.^{27} The total electron count and the void volume suggest the presence of two additional toluene molecules in the asymmetric unit. Their contribution to the total structure factor has been calculated and incorporated in the subsequent least-squares refinements of the main residues.

Crystal data for **5**. C$_{36}$H$_{39}$IrP$_2$; *M* = 725.81; yellow prism, 0.067 x 0.072 x 0.166 mm^3; orthorhombic *Pbca*; *a* = 16.5310(10), *b* = 18.3871(12), *c* = 20.0878(13) Å; *V* = 6105.8(7) Å^3; *Z* = 8; ρ_{calc} = 1.579 g cm^{-3}; μ = 4.502 cm^{-1}; min. and max. transmission factors 0.619 and 0.716; 2θ$_{max}$ = 55.786°; 92015 reflections collected; 7078 unique reflections [R_{int} = 0.0776]; number of data/restraints/parameters: 7078/0/396; final *GOF* 1.067; R_1 = 0.0273 [4854 reflections, *I* > 2σ(*I*)], wR_2 = 0.0576 for all data; largest difference peak: 1.101 e Å^{-3}. Hydride ligand was included in the model in observed position and freely isotropically refined.

Crystal data for **7·NH$_3$**. C$_{35}$H$_{40}$IrNP·NH$_3$; *M* = 745.85; yellow prism, 0.218 x 0.224 x 0.231 mm^3; monoclinic *P2$_1$/c*; *a* = 10.3409(4), *b* = 16.3633(7), *c* = 18.3773(8) Å, β = 103.7330(10)°; *V* = 3020.7(2) Å^3; *Z* = 4; ρ_{calc} = 1.640 g cm^{-3}; μ = 4.554 cm^{-1}; min. and max. transmission factors 0.349 and 0.486; 2θ$_{max}$ = 59.348°; 63860 reflections collected; 8179 unique reflections [R_{int} = 0.0413]; number of data/restraints/parameters: 8179/2/513; final *GOF* 1.130; R_1 = 0.0221 [7300 reflections, *I* > 2σ(*I*)], wR_2 = 0.0572 for all data; largest difference peak: 1.411 e Å^{-3}. Hydrogen atoms of amido fragment have been observed in Fourier difference maps; however they have not been included in the model as their refinement does not converge and lead to very short H···H distances. Hydrogen atoms of ammonia have neither been observed nor included in the model.

Computational Details

All DFT theoretical calculations have been carried out using the Gaussian program package.^{28} The B3LYP method^{29} has been

employed including the D3 dispersion correction scheme developed by Grimme for both energies and gradient calculations and the "ultrafine" grid.[30] The def2-SVP basis set[31] has been selected for all atoms. Energies have been refined by single point calculations using the def2-TZVP basis set and the PCM method[32] for simulation of solvent effects (toluene, ε = 2.3741). Gibbs energy corrections have been calculated at 298 K and 1 atm. The nature of the stationary points has been check by analytical frequency analysis and transition states were characterized by a single imaginary frequency corresponding to the expected motion of the atoms.

Acknowledgements

Notes and references

1   a) T. Braun, *Angew. Chem. Int. Ed.*, 2005, **44**, 5012–5014; J. I. van der Vlugt, *Chem. Soc. Rev.*, **2010**, *39*, 2302–2322; b) J. L. Klinkenberg and J. F. Hartwig, *Angew. Chem. Int. Ed.*, 2011, **50**, 86–95; c) J. Kim, H. J. Kim and S. Chang, *Eur. J. Org. Chem.*, 2013, 3201–3213.

2   a) J. Zhao, A. S. Goldman and J. F. Hartwig, *Science*, 2005, **307**, 1080–1082; b) E. Morgan, D. F. MacLean, R. McDonald and L. Turculet, *J. Am. Chem. Soc.*, 2009, **131**, 14234–14236.

3   E. Khaskin, M. A. Iron, L. J. W. Shimon, J. Zhang and D. Milstein, *J. Am. Chem. Soc.*, 2010, *132*, 8542–854.

4   a) Y. H. Chang, Y. Nakajima, H. Tanaka, K. Yoshizawa and F. Ozawa, *J. Am. Chem. Soc.*, 2013, **135**, 11791–11794; b) H. –O. Taguchi, D. Sasaki, K. Takeuchi, S. Tsujimoto, T. Matsuo, H. Tanaka, K. Yoshizawa and F. Ozawa, *Organometallics*, 2016, **35**, 1526–1533.

5   a) D. V. Gutsulyak, W. E. Piers, J. Borau-Garcia and M. Parvez, *J. Am. Chem. Soc.*, 2013, **135**, 11776–11779; b) R. M. Brown, J. B. Garcia, J. Valjus, C. J. Roberts, H. M. Tuononen, M. Parvez and R. Roesler, *Angew. Chem. Int. Ed.*, 2015, **54**, 6274–6277.

6   a) Y. Kim and S. Park, *C. R. Chemie*, 2016, **19**, 614–629; b) M. G. Scheibel, J. Abbenseth, M. Kinauer, F. W. Heinemann, C. Würtele, B. de Bruin, S. Schneider. *Inorg. Chem.* **2015**, *54*, 9290–9302; c) J. Cámpora, P. Palma, D. del Río, M. M. Conejo and E. Álvarez, *Organometallics*, **2004**, *23*, 5653–5655; d) D. J. Fox, R. G. Bergman, *J. Am. Chem. Soc.* **2003**, *125*, 8984–8985; e) A. W. Kaplan, J. C. M. Ritter, R. G. Bergman, *J. Am. Chem. Soc.* **1998**, *120*, 6828–6829; f) D. Conner, K. N. Jayaprakash, T. R. Cundari, T. B. Gunnoe, *Organometallics* **2004**, *23*, 2724–2733; g) A.W. Holland, R. G. Bergman, *J. Am. Chem. Soc.* **2002**, *124*, 14684–14695; h) K. N. Jayaprakash, D. Conner, T. B. Gunnoe, *Organometallics* **2001**, *20*, 5254–5256.

7   a) D. K. N. Conner, T. R. Jayaprakash, T. B. Cundari, T. B. Gunnoe, *Organometallics* **2004**, *23*, 2724–2733; b) F. L. Joslin, M. P. Johnson, J. T. Mague, D. M. Roundhill, *Organometallics* **1991**, *10*, 2781–2794; c) D. J. Fox, R. G. Bergman, *Organometallics* **2004**, *23*, 1656–1670; d) D. Conner, K. N. Jayaprakash, M. B. Wells, S. Manzer, T. B. Gunnoe, P. D. Boyle, *Inorg. Chem.* **2003**, *42*, 4759–4772; e) J. R. Fulton, S. Sklenak, M. W. Bouwkamp, R. G. Bergman, *J. Am. Chem. Soc.* **2002**, *124*, 4722–4737; f) J. R. Fulton, M. W. Bouwkamp, R. G. Bergman, *J. Am. Chem. Soc.* **2000**, *122*, 8799–8800.

8   D. J. Fox, R. G. Bergman, *J. Am. Chem. Soc.* **2003**, *125*, 8984–8985.

9   M. Kanzelberger, X. Zhang, T. J. Emge, A. S. Goldman, J. Zhao, C. Incarvito, J. F. Hartwig, *J. Am. Chem. Soc.* **2003**, *125*, 13644–13645.

10 a) P. S. Hanley, J. F. Hartwig, *Angew. Chem. Int. Ed.*, 2013, **52**, 8510–8525; b) J. W. Tye, J. F. Hartwig, *J. Am. Chem. Soc.* **2009**, *131*, 14803–14712.

11 a) T. Kimura, H. Arita, K. Ishiwata, S. Kuwata, T. Ikariya, *Dalton Trans.* **2009**, 2912–2914; b) A. L. Casalnuovo, J. C. Calabrese, D. Milstein, *Inorg. Chem.* **1987**, *26*, 971–973; c) R. Koelliker, D. Milstein, *Angew. Chem., Int. Ed. Engl.* **1991**, *30*, 707–709; d) M. A. Salomon, A. K. Jungton, T. Braun, *Dalton Trans.* **2009**, 7669–7677; e) T. Kimura, N. Koiso, K. Ishiwata, S. Kuwata, T. Ikariya, *J. Am. Chem. Soc.* **2011**, *133*, 8880–8883; f) P. Kläring, S. Pahl, T. Braun, A. Pennera, *Dalton Trans.* **2010**, 6785–6791.

12 a) I. Mena, M. A. Casado, P. García-Orduña, V. Polo, F. J. Lahoz, A. Fazal, L. A. Oro, *Angew. Chem. Int. Ed.* **2011**, *50*, 11735–11738; b) E. Vélez, M. P. Betoré, M. A. Casado, V. Polo, *Organometallics* **2015**, *34*, 3959–3966.

13 a) I. Mena, E. A. Jaseer, M. A. Casado, P. García-Orduña, F. J. Lahoz, L. A. Oro, *Chem. Eur. J.* **2013**, *19*, 5665–5675; b) I. Mena, M. A. Casao, V. Polo, P. García-Orduña, F. J. Lahoz, L. A. Oro, *Dalton Trans.* **2014**, *43*, 1609–1619.

14 I. Mena, M. A. Casado, V. Polo, P. García-Orduña, F. J. Lahoz, L. A. Oro, *Angew. Chem. Int. Ed.* **2012**, *51*, 8259–8263.

15 I. Mena, M. A. Casado, V. Polo, P. García-Orduña, F. J. Lahoz, L. A. Oro, *Angew. Chem. Int. Ed.* **2014**, *53*, 9627–9631.

16 a) H. –H. Wang, L. H. Pignolet, P. E. Reedy, Jr., M. M. Olmstead, A. L. Balch, *Inorg. Chem.* **1987**, *26,* 377–383; b) T. Lumini, G. Laurenczy, R. Roulet, A. Tassan, R. Ros, K. Schenk, *Helv. Chim. Acta* **1998**, *81,* 781–791; c) R. Ros, A.–Tassan, S. Detti, R. Roulet, K. Schenk, *Inorg. Chim. Acta* **2006**, *359*, 2417–2423.

17 a) M. A. Esteruelas, M. Oliván, L. A. Oro, M. Schulz, E. Sola, H. Werner, *Organometallics* **1992**, *11,* 3659–3664; b) M. Martín, E. Sola, O. Torres, P. Plou, L. A. Oro, *Organometallics* **2003**, *22,* 5406–5417; b) M. Martín, O. Torres, E. Oñate, E. Sola, L. A. Oro, *J. Am. Chem. Soc.* **2005**, *127,* 18074–18084; c) J. S. Merola, M. A. Franks, *J. Organomet. Chem.* **2013**, *723*, 49–55; d) S. M. W. Rahaman, S. Dinda, A. Sinha, J. K. Bera, *Organometallics* **2013**, *32*, 192–201; e) B. Raible, V. Gierz, D. Kunz, *Organometallics* **2015**, *34*, 2018–2027.

18 T. C. Bianchini, E. Farnetti, M. Graziani, G. Nardin, A. Vacca, F. Zanobini, *J. Am. Chem. Soc.* **1990**, *112*, 9190–9197.

19 G. W. Bushnell, M. A. Casado, S. R. Stobart, *Organometallics*, **2001**, *20*, 601–603.

20 M. R. Churchill, S. A. Bezman, *Inorg. Chem.* **1973**, *12,* 531–536.

21 J. Schöffel, A. Y. Rogachev, S. D. George, P. Burger, *Angew. Chem. Int. Ed.* **2009**, *48,* 4734–4738.

22 D. Rais, R. G. Bergman, *Chem. Eur. J.* **2004**, *10,* 3970–3978.

23 SAINT+, version 6.01: Area-Detector Integration Software, Bruker AXS, Madison, 2001.

24 R. H. Blessing, *Acta Crystallogr.* **1995**, *A51*, 33–38; SADABS, Area Detector Absorption Correction Program, Bruker AXS, Madison, WI, 1996.

25 a) G. M. Sheldrick, *Acta Crystallogr.* **1990**, *A46*, 467–473; b) G. M. Sheldrick, *Acta Crystallogr.* **2008**, *A64*, 112–122.

26 G. M. Sheldrick, *Acta Crystallogr.* **2015**, *C71*, 3–8.

27 A. L. Spek, *Acta Crystallogr.* **2015**, *C71*, 9–18.

28 M. J. Frisch, G. W. Trucks, H. B. Schlegel, G. E. Scuseria, M. A. Robb, J. R. Cheeseman, G. Scalmani, V. Barone, B. Mennucci, G. A. Petersson, H. Nakatsuji, M. Caricato, X. Li, H. P. Hratchian, A. F. Izmaylov, J. Bloino, G. Zheng, J. L. Sonnenberg, M. Hada, M. Ehara, K. Toyota, R. Fukuda, J. Hasegawa, M. Ishida, T. Nakajima, Y. Honda, O. Kitao, H. Nakai, T. Vreven, J. A. Montgomery Jr, J. E. Peralta, F. Ogliaro, M. Bearpark, J. J. Heyd, E. Brothers, K. N. Kudin, V. N. Staroverov, R. Kobayashi, J. Normand, K. Raghavachari, A. Rendell, J. C. Burant, S. S. Iyengar, J. Tomasi, M. Cossi, N. Rega, J. M. Millam, M. Klene, J. E. Knox, J. B. Cross, V. Bakken, C. Adamo, J. Jaramillo, R. Gomperts, R. E. Stratmann, O. Yazyev, A. J. Austin, R. Cammi, C. Pomelli, J. W. Ochterski, R. L. Martin, K. Morokuma, V. G. Zakrzewski, G. A. Voth, P. Salvador, J. J.

Dalton Transactions Accepted Manuscript

ARTICLE

Dannenberg, S. Dapprich, A. D. Daniels, ¨O. Farkas, J. B. Foresman, J. V. Ortiz, J. Cioslowski, D. J. Fox, Gaussian, Inc., Wallingford CT, **2013**.

29   a) C. Lee, W. Yang, R. G. Parr, *Phys. Rev. B.* **1998**, *37*, 785–789; b) A. D. Becke, *J. Chem. Phys.* **1993**, *98*, 1372–1377; c) A. D. Becke, *J. Chem. Phys.* **1993**, *98*, 5648–5652.

30   S. Grimme, J. Antony, S. Ehrlich, H. Krieg, *J. Chem. Phys.* **2010**, *132*, 154104.

31   F. Weigend, R. Ahlrichs, *Phys. Chem. Chem. Phys.* **2005**, 7, 3297–3305.

32   J. Tomasi, B. Mennucci, R. Cammi, *Chem. Rev.* **2005**, *105*, 2999–3094.

Dalton Transactions Accepted Manuscript

The −NH$_2$ bridges in polynuclear diolefin complexes of iridium are split into mononuclear terminal amido complexes in the presence of bis(phosphanes). The tfbb-containing species evolve by forming a C−NH$_2$ bond between the amido moiety and the coordinated diene, while the cod complexes undergo extrusion of ammonia by C-H activation.

Dalton Transactions Accepted Manuscript